Annals of Glaciology 32 2001

Simulating snowmelt processes during rain-on-snow over a semi-arid mountain basin

Danny Marks,[1] Tim Link,[2] Adam Winstral,[1] David Garen[3]
[1]*USDA Agricultural Research Service, Northwest Watershed Research Center, Boise, ID 83712-7716, U.S.A.*
[2]*Oregon State University, Corvallis, OR 97331-2130, U.S.A.*
[3]*USDA Natural Resources Conservation Service, Western Climate Center, Portland, OR 97204-3224, U.S.A.*

ABSTRACT. In the Pacific Northwest of North America, significant flooding can occur during mid-winter rain-on-snow events. Warm, wet Pacific storms caused significant floods in the Pacific Northwest in February 1996, January 1997 and January 1998. Rapid melting of the mountain snow cover substantially augmented discharge during these flood events. An energy-balance snowmelt model is used to simulate snowmelt processes during the January 1997 event over a small headwater basin within the Reynolds Creek Experimental Watershed located in the Owyhee Mountains of southwestern Idaho, U.S.A. This sub-basin is 34% forested (12% fir, 22% aspen and 66% mixed sagebrush (primarily mountain big sagebrush)). Data from paired open and forested experimental sites were used to drive the model. Model-forcing data were corrected for topographic and vegetation canopy effects. The event was preceded by cold, stormy conditions that developed a significant snow cover over the sub-basin. The snow cover at sites protected by forest cover was slightly reduced, while at open sites significant snowmelt occurred. The warm, moist, windy conditions during the flooding event produced substantially higher melt rates in exposed areas, where sensible- and latent-heat exchanges contributed 60–90% of the energy for snowmelt. Simulated snow-cover development and ablation during the model run closely matched measured conditions at the two experimental sites. This experiment shows the sensitivity of snowmelt processes to both climate and land cover, and illustrates how the forest canopy is coupled to the hydrologic cycle in mountainous areas.

INTRODUCTION

In the Pacific Northwest of North America significant flooding can occur during mid-winter rain-on-snow events. During rain-on-snow the potential for flooding is increased if the soil is frozen (Dunne and Black, 1971; Seyfried and others, 1990; Seyfried and Flerchinger, 1994; Shanley and Chalmers, 1999), if the snow cover extends over the whole basin (especially to lower elevations) and if the storm event is accompanied by high winds. As shown by Marks and others (1998), high winds during rain-on-snow events increase turbulent transfer at the snow surface, causing condensation and subsequent snowmelt. Increases in sensible- and latent-heat exchanges can significantly increase the snowmelt contribution to water available for runoff (WAR) during the event, leading to extensive sediment transport (Seyfried and Flerchinger, 1994; Shanley and Chalmers, 1999), landsliding (Orme, 1989) and flooding (Marks and others, 1998).

Forest and vegetation cover will increase snow-cover shading, increase thermal radiation input, decrease air temperatures and reduce wind speeds (Link and Marks, 1999a, b). The overall effect is a dampening of energy-flux magnitudes during periods of high wind as compared to open sites. During warm, windy, rain-on-snow events, sheltered areas have lower melt rates, generating less WAR than nearby exposed areas with similar snow cover. Link and Marks (1999a) showed that if general vegetation characteristics of canopy shape, height and crown closure are specified, snow deposition and melt can be accurately simulated over large regions with heterogeneous vegetation cover. Marks and others (in press) used data from an exposed and a forested site to accurately simulate snow deposition and melt over several snow seasons at two contrasting sites in the Reynolds Mountain East (RME) sub-basin of the Reynolds Creek Experimental Watershed (RCEW) (239 km^2) located in the Owyhee Mountains in Idaho, U.S.A. They showed that the effect of vegetation cover significantly alters both the deposition and melt patterns of the seasonal snow cover and that the most critical difference between the sites was increased wind speeds at the exposed site.

In this study we investigate the spatial patterns of the generation of snowmelt and WAR during a rain-on-snow event that occurred over a 3 day period from 31 December 1996 to 2 January 1997 in the same headwater sub-basin (RME) of RCEW that was the subject of point analysis by Marks and others (in press). During the event, 81 mm of precipitation fell (most of it as rain) on the RME research area (0.36 km^2). The snow cover was nearly depleted in exposed areas of the basin, as 130 mm of snowmelt and 184 mm of WAR (snowmelt plus rain that passed through the snow cover) were generated and stream discharge increased 50-fold from a daily flow of < 0.5 mm on 28 December to 26 mm on 2 January.*

* Values for snowmelt and WAR over the RME basin, and stream discharge through the RME weir are given as a *specific discharge*, which is defined as a depth of water over the basin area in mm. It is used so that discharge through the weir can be directly compared to precipitation, snowmelt and WAR at the soil surface.

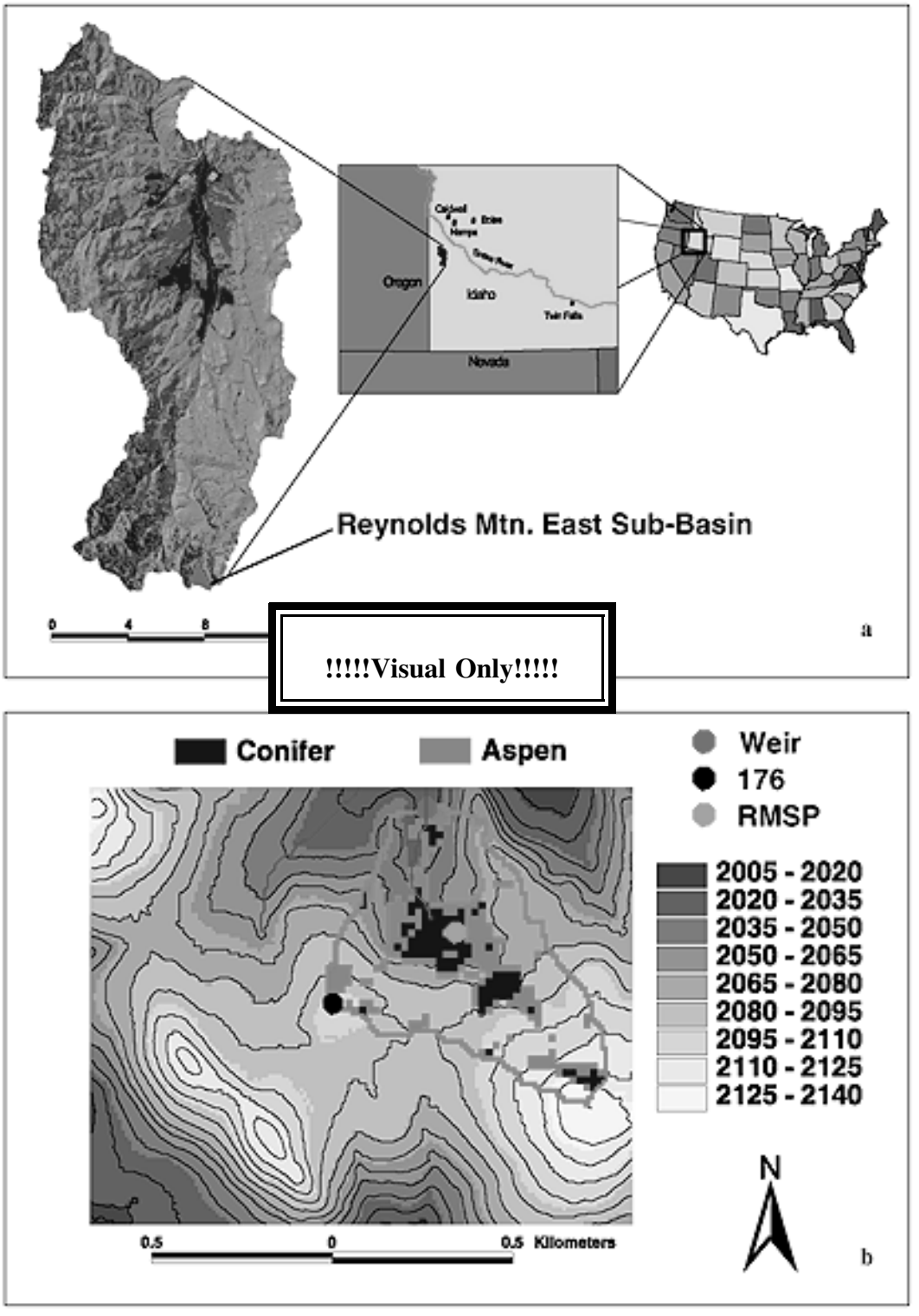

Fig. 1. Location of RCEW (a), and map of the RME study area showing topography, location of measurement sites, weir and vegetation communities (b).

Vegetation distribution, topography and climate data from the exposed and sheltered weather stations in the RME sub-basin are used to develop distributed fields of climate (air temperature, humidity, wind, solar and thermal radiation, soil temperature and precipitation) over the RME headwater basin, for 1 October 1996 through 1 March 1997. These climate fields were used as forcing data for a topographically distributed energy-balance snowmelt model ISNOBAL (Marks and others, 1999). Results from the simulation are used to show how topographic structure and vegetation cover influence the generation of snowmelt and runoff from the base of the snow cover, or WAR, during a rain-on-snow event.

THE STUDY SITE

RCEW

RCEW was established in 1960 by the United States Department of Agriculture (USDA) Agricultural Research Service (ARS) as a field laboratory for hydrologic research to address water-resource issues and validate hydrologic

models (Robins and others, 1965). Research in RCEW has provided information to help solve critical water-supply, water-quality and rangeland management problems in the northwestern U.S. for the past 40 years.

The RCEW watershed (239 km^2) is located on the northern flank of the Owyhee Mountains in southwestern Idaho, approximately 65 km southwest of Boise (Fig. 1a). Reynolds Creek is a perennial stream that drains north to the Snake River. RCEW ranges in elevation from 1101 to 2241 m. About 77% of the watershed is under federal or state ownership, with the remainder being privately owned. Primary land use in the watershed is livestock grazing, with some irrigated fields along the creek at lower elevations. Extensive hydro-climatic records (precipitation, temperature, humidity, wind, snow depth and water equivalent, soil temperature and moisture and streamflow) have been collected in the watershed since the early 1960s. Average annual precipitation varies from about 225 mm at the lower elevations, to >1100 mm at the ridge tops at the southern end of the watershed. Average annual stream discharge from the outflow of RCEW is 75 mm m^{-2}, while from RME, a 0.36 km^2 headwater sub-basin located at the southern end of RCEW (see Fig. 1a and b), it is 584 mm m^{-2}.

Experimental sub-basin

The RME sub-basin (2027–2137 m a.s.l.) was used for this study. Mountain big sage, aspen and mixed conifer are the dominant plant communities. About 34% of the RME sub-basin is forested (12% mixed conifer (shown in Fig. 1b as dark green), and 22% aspen (shown as light green)), and 66% is a mixed sagebrush (in Fig. 1b all the area inside the RME sub-basin that is neither dark nor light green).

Two climate stations were used to develop the distributed climate fields for this study, the Reynolds Mountain Climate Station (site 176) and the Reynolds Mountain Snow Pillow (RMSP) site. Both are located within the RME sub-basin. Site 176 (2097 m) is an open site located on a broad shelf on the southwestern edge of RCEW with an unobstructed fetch for several km to the southwest, the prevailing wind direction. Site 176 is the primary upper climate-monitoring station for RCEW, and has been in operation since 1962, providing hourly data on air temperature, humidity, wind, solar radiation, soil temperature and precipitation. The RMSP site (2073 m) is located within a fir and aspen grove, below and just in the lee of the ridge upon which site 176 is located. It is the primary snow-study plot for RCEW, and has been in operation since 1968, providing hourly data on air temperature, humidity, wind, solar radiation, soil temperature, precipitation and snow water equivalent (SWE) from both a snow pillow and regular snow courses. Stream discharge from the RME sub-basin has been measured continuously with a 90° V-notch weir at its outflow since 1963 (Fig. 1b).

MODEL DESCRIPTION

In a seasonal snow cover, snow continuously experiences thermodynamic changes, undergoing continuous metamorphism until it melts and becomes available for runoff during spring (Colbeck, 1982). These metamorphic changes and the final melting are driven by temperature and vapor-density gradients within the snow cover, which are caused by heat exchange at the snow surface and at the snow–soil interface (Colbeck and others, 1979; Male and Granger, 1981). In general, the energy balance of a snow cover is expressed as

$$\Delta Q = R_{\mathrm{n}} + H + L_{\mathrm{v}}E + G + M, \qquad (1)$$

where ΔQ is change in snow-cover energy and $R_{\mathrm{n}}, H, L_{\mathrm{v}}E, G$ and M are net radiative, sensible, latent, conductive and advective energy fluxes (all terms are in W m^{-2}). In thermal equilibrium, $\Delta Q = 0$; a negative energy balance will cool the snow cover, increasing its "cold" content,* while a positive energy balance will warm the snow cover. The snow cover cannot be warmer than 0.0°C, and melt cannot occur in significant amounts until the entire snow cover has reached this temperature. Once the entire snow cover is isothermal at 0.0°C, positive values of ΔQ must result in melt (Anderson, 1976; Marks and Dozier, 1992).

A snow-cover energy and mass-balance model ISNOBAL developed by Marks and others (1999) was used for the analysis presented in this paper. The model is designed to be run over a digital elevation model (DEM) grid, solving the snow-cover energy balance, calculating snowmelt and runoff from the base of the snow cover (WAR) at each gridcell. ISNOBAL uses initial conditions of topographic structure, surface roughness and climate-measurement heights, with climate-forcing data at each time-step and precipitation data at each occurrence to predict the accumulation and ablation of the snow cover at each DEM gridcell over the simulation area. The state and forcing variables are presented in Table 1.

The model approximates the snow cover as being composed of two layers, a surface fixed-thickness active layer and a lower layer, solving for the temperature (°C) and specific mass (kg m^{-2}) or depth of water equivalent per unit area (mm m^{-2}) for each.

Melt is computed in either layer when the accumulated energy exceeds the "cold" content or when the computed "cold" content is >0.0. Runoff from the base of the snow cover is computed when the accumulated melt and liquid H_2O content of the snow cover exceed a specified threshold. This threshold is a volume ratio defined as the maximum liquid-water retention capacity and is based on the work of

Table 1. State variables predicted by, and forcing variables required by, the ISNOBAL topographically distributed snowmelt model

State variables	*Forcing variables*
Snow depth (m)	Net solar radiation (W m^{-2})
Snow density (kg m^{-3})	Incoming thermal radiation (W m^{-2})
Snow surface layer temperature (°C)	Air temperature (°C)
Average snow-cover temperature (°C)	Vapor pressure (Pa)
Average snow liquid-water content (%)	Wind speed (m s^{-1})
	Soil temp. (°C)
	Precipitation (mm)

* The "cold" content of a snow cover is defined as the amount of energy in J m^{-2} required to bring its temperature to 0.0°C. Though the internal energy of the snow cover would correctly be referred to as its "heat" content, snow hydrologists use "cold" content as a convenient way of assessing the relative condition of the snow cover in regard to reaching 0.0°C which must be achieved before melt can begin.

Davis and others (1985) and may have a range of values depending on conditions.

A detailed description of the equations solved within the model is presented by Marks and others (1998), who developed SNOBAL, the point version of ISNOBAL, to simulate snowmelt during a rain-on-snow event that caused extensive flooding in the Oregon Cascades during February 1996. SNOBAL was also used by Link and Marks (1999b) to simulate the dynamics of the snow cover beneath boreal forest canopies in northern Canada.

ISNOBAL is a grid-based version of SNOBAL that solves an identical set of equations and uses the same subroutine library. It is described in detail by Marks and others (1999) who used it to simulate the development and ablation of the seasonal snow cover over the Wasatch Mountains, Utah, U.S.A., for the 1994 and 1995 snow seasons. Link and Marks (1999a) used ISNOBAL to simulate the effects of canopy cover on snow deposition and melt in boreal Canada. The software and detailed descriptions of both models are available from D. Marks (http://www.nwrc.ars.usda.gov/ipw).

RAIN-ON-SNOW EVENT

During a 3 day period from 31 December 1996 to 2 January 1997, a warm storm deposited 35–145 mm of rain over RCEW, based on data from the 16 precipitation sites and four climate stations in RCEW. This event melted a large part of the snow cover, which contributed to a significant increase in discharge throughout RCEW. Two of the ten largest single-day discharges from the RCEW outlet weir since 1962 (5.2 mm or 14.46 $m^3 s^{-1}$ on 1 January 1997, and 5.5 mm or 15.24 $m^3 s^{-1}$ on 2 January 1997) were recorded during this event.

In the RME sub-basin, 81 mm of precipitation (most of which was rain) fell during the same period. This precipitation combined with high snowmelt rates to generate significant discharge at the RME weir as well. The RME weir, which has a January average daily discharge of <0.1 mm (approximately 0.5 $L s^{-1}$), recorded 12 mm (60 $L s^{-1}$) of discharge on 1 January 1997, 26 mm (130 $L s^{-1}$) on 2 January 1997, and 14 mm (70 $L s^{-1}$) on 3 January 1997. Over 120 mm of discharge flowed through the weir during January 1997.

SNOW-COVER SIMULATION

Development of the seasonal snow cover in the upper elevations of RCEW began in early November 1996, with the snow cover extending to mid-elevations by mid-November. In early December a series of cold storms extended the snow cover over much of the RCEW basin. In mid-December the RME sub-basin was completely covered by >1 m of snow. Several large drifts and areas protected by forest cover held substantially more snow.

The topographically distributed snowmelt model ISNOBAL (Marks and others, 1999) was used to simulate the development and ablation of the snow cover over the RME sub-basin from 1 October 1996 to 1 March 1997. The area containing the RME sub-basin was represented using a 10 m DEM grid, containing 88 rows and 80 columns, giving a total of 7040 gridcells. The RME sub-basin within this grid consisted of 3762 gridcells.

Data from the two experimental sites (Fig. 1b) were used to develop hourly input grids of net solar radiation, incoming thermal radiation, air temperature, vapor pressure, soil temperature and wind speed (see Table 1). Input files were prepared using the methods described by Susong and others (1999). Clear-sky solar and thermal radiation were calculated and corrected for topographic effects of slope, aspect, horizon effects and shading from adjacent terrain, using methods described by Marks and Dozier (1979), Dozier (1980) and Dubayah and others (1990). Clear-sky radiation was corrected for cloud cover using measured values from the measurement sites within the RME sub-basin and for canopy effects using methods described by Link and Marks (1999a, b). Net solar radiation was calculated from cloud- and canopy-corrected solar irradiance and topographically corrected snow albedo (Marks and others, 1999; Susong and others, 1999).

Air temperature, vapor pressure and soil temperature were distributed over the DEM grid using data from the measurement sites and a simple linear distribution with elevation. Wind-speed grids were derived from site data, topographic structure and canopy shelter, using exposure/shelter parameters developed by Winstral (1999). Topographic structure relative to long-term wind direction, canopy cover and long-term wind-speed differences between the protected RMSP site and the exposed 176 site were used to develop a wind-factor field for the RME sub-basin. Hourly wind data from the two meteorological stations were interpolated over the wind-factor field to derive hourly wind-speed grids. The distributed wind fields were then combined with long-term solid-precipitation accumulation differences between the two measurement sites (Marks and others, in press) to distribute precipitation mass across the study basin. Relative to the representative sheltered regions (e.g. site RMSP), snow accumulation was further enhanced within modeled drift zones. These were modeled using terrain parameters that describe upwind

Table 2. Measured and simulated mass summary, rain-on-snow event, 28 December 1996 through 4 January 1997, RME sub-basin

	28 Dec.	*29 Dec.*	*30 Dec.*	*31 Dec.*	*1 Jan.*	*2 Jan.*	*3 Jan.*	*4 Jan.*
Measured:								
Snow pillow SWE (mm)	530	550	540	600	555	500	510	510
Simulated:								
SWE (mm, conifers)	497	527	520	506	498	501	521	522
SWE (mm, RME basin)	409	417	404	369	339	340	357	357
Measured:								
Weir discharge (mm)	0	0	1	1	12	26	14	9
Simulated:								
Average WAR (mm)	0	23	14	41	75	13	0	0

breaks in slope (Winstral, 1999) and showed excellent agreement with late-season aerial assessments of snow-covered area from previous years.

Forcing the 151 day ISNOBAL simulation (1 October–1 March) required 3624 ten-band input images and 667 four-band precipitation images (just over 200 MB of input files). Snow-cover initialization was set to zero, as the run began on 1 October. Under these conditions, ISNOBAL will simulate the development of the snow cover over the basin based on weather conditions and precipitation. The simulation, which took 2 h 15 min of central processing unit time on a standard desktop workstation, generated 151 (one per day) ten-band energy-balance images containing net all-wave radiation (R_n), sensible (H), latent (L_vE), soil (G) and advected (M) heat fluxes, the energy-balance sum ΔQ, total evaporative flux, snowmelt, runoff from the base of the snow cover and snow-cover cold content and 151 nine-band snow-cover mass images containing snow depth, density, mass (SWE), liquid-water content, temperature of the upper, lower and entire snow cover, lower layer thickness and per cent liquid-water saturation. A detailed discussion of the model, its input and initialization requirements and its outputs as well as all of the utilities used to generate the input files is presented by D. Marks (http://www.nwrc.ars.usda.gov/ipw).

Simulation results

Table 2 presents measured and simulated snow-cover mass, simulated WAR and measured discharge at the RME weir during the event. Data from a snow pillow at the RMSP site, located in an opening in a grove of fir trees, were available during the event. The SWE measured by the snow pillow at the end of each day from 28 December to 4 January is compared to the average SWE from the 452 gridcells within the conifer class (12% of the basin) in the RME sub-basin. In general, the trends in SWE shown by the snow pillow are followed by simulated SWE in the conifers. The snow cover in the conifers was deeper and cooler than in much of the rest of the basin, producing less snowmelt and WAR during the event. As a result, measured and simulated SWE did not change significantly during the event. Measured SWE was 530 mm on 28 December and 510 mm on 4 January, a decrease of 20 mm, while simulated SWE in the conifers was 497 mm on 28 December and 522 mm on 4 January, an increase of 25 mm. In contrast, the average simulated SWE over the whole RME sub-basin was 409 mm on 28 December and 357 mm on 4 January, a loss of 52 mm during the event.

The increase in SWE over the snow pillow shown in Table 2 on 31 December and 1 January is an artifact of what happens to a snow pillow at the onset of a rain-on-snow event. Soil temperatures over much of the RME sub-basin were above freezing prior to the event, adding energy to the snow cover and allowing most of the rain to pass through the snow cover. Snow temperatures above snow pillows tend to be much colder than those above soil, however, due in part to the insulating properties of the pillow itself and because the pillow blocks the exchange of water vapor between the soil and the snow. The initial pulse of rainwater through the snow cover tends to be held in this cold layer above the pillow, increasing the measured SWE, until the temperature gradient is eliminated. Once the impeded rainwater begins to flow from above the snow pillow, it can have a "flushing" effect, causing a sudden downward spike in SWE over the pillow that is not manifest in snow over ground. This phenomenon was observed at numerous snow-pillow sites in the Cascade Mountains of Oregon during a rain-on-snow event in February 1996, by Marks and others (1998).

Table 2 also compares measured discharge through the weir to average simulated WAR over the RME sub-basin. Measured discharge from the RME sub-basin totaled 5 mm in October, 13 mm in November and 11 mm in December, values which are all close to the 35 year monthly averages for the RME sub-basin. Prior to the event, measured daily discharge was essentially zero (i.e. $<0.1\,\mathrm{mm\,d^{-1}}$). Soils in the basin are about 1 m deep and have a water-holding capacity of about 25%, or 250 mm. The period October–December 1996 was relatively warm and wet, leaving the soils in a thawed, moist state. Weir discharge began to respond to the rain-on-snow event on 1 January 1997, jumping to a daily total of 12 mm, and reached a peak daily total of 26 mm on 2 January. By the end of January, a total of > 120 mm (about 10 times the average January value) of discharge had passed through the RME weir. Another 38 mm (4 times the monthly average) occurred in February, bringing the 2 month total to 158 mm.

Simulated WAR from the snow cover for the event began on 29 December with a total of 23 mm, increased on 31 December to a total of 41 mm and on 1 January reached a peak of 75 mm. The total simulated WAR from the snow cover was 166 mm from 29 December to 2 January. The transition from WAR to discharge through the weir is a complicated process involving infiltration, both shallow and deep storage and both surface and subsurface flow while moving toward the stream channel and finally to the weir. It is therefore unreasonable to expect simulated WAR to match measured discharge at the RME weir in either absolute timing or magnitude over a period of a few days or weeks. As Table 2 illustrates, however, after an initial lag of a few days, the weir discharge responds fairly rapidly to the rain-on-snow event, and over the month of January simulated WAR (166 mm) was similar to measured discharge (120 mm).

Terrain and vegetation effects

The RME sub-basin was divided into three vegetation classes (see Fig. 1b) for the simulation. The high canopy heights and dense crown closure of the conifer class produce increased shading and thermal emissivity and decreased wind speeds. Conversely, the sage class provides little shading or emissivity enhancement and no wind reduction. The aspen class provides some shading, emissivity enhancement and wind reduction.

Terrain and vegetation were combined to estimate distributed wind fields and wind effects on snow deposition, using methods described by Winstral (1999) for terrain-induced wind effects and Link and Marks (1999a, b) for vegetation effects. Wind exposure and snow-deposition enhancement (drifting) was continuously distributed over the watershed, to simulate scour and drift development during snow deposition. To further analyze the simulation results, terrain and canopy effects on wind and precipitation were combined to produce four accumulation/exposure regimes: (1) topographically exposed areas, (2) topographically sheltered or fir-covered areas, (3) drift areas, and (4) the rest of the basin. Exposed areas (class 1 above) are areas with little or no up-wind topographic shelter and were exclusively in the sage vegetation class. Sheltered areas (class 2) are areas with either topographic sheltering above or fir forest cover. Most, though not all, of the aspen vegetation class fell into this category. Drift areas (class 3) were

Table 3. Simulated SWE by vegetation and wind-exposure class, rain-on-snow event, 30 December 1996 through 3 January 1997

	30 Dec.		*2 Jan.*		*3 Jan.*	
Conifer (12%)	522	14%	500	18%	523	17%
Aspen (22%)	485	27%	436	28%	456	28%
Sage (66%)	358	59%	281	54%	296	55%
Exposed (14%)	86	3%	0	0%	8	0%
Sheltered (17%)	434	18%	417	21%	435	21%
Drift zone (15%)	1160	44%	1147	50%	1186	50%
"The rest" (54%)	261	35%	177	28%	185	28%
RME basin (100%)	404		340		357	

Notes: Figures in parentheses indicate the percentage of the area of RME occupied by that class. Other percentages indicate the percentage of the total SWE over the RME basin in that class.

sheltered areas with an upwind slope break of $> 7^{\circ}$. Class 4 was everything not in classes 1–3 and was mostly in the sage vegetation class, with a small amount of aspen.

Table 3 presents simulated SWE by vegetation and wind-exposure class throughout the event. The percentages next to the class titles represent the class proportion of the total basin, and percentages next to the SWE values represent class proportion of total basin SWE

At the start of the event on 30 December 1996, there was a simulated basin average SWE of 404 mm, with 14% of the total beneath conifers, 27% of the total beneath aspens and 59% of the total over sage. The forested areas had slightly more SWE than their representative areas, and the sage slightly less.

At the end of 2 January 1997, when basin-wide SWE was at its event minimum, there was 340 mm of SWE covering the basin, of which 18% was beneath conifers, 28% beneath aspens and 54% over the sage. Though SWE in all vegetation classes decreased, the percentage of basin SWE beneath conifers had increased, while the proportion of basin SWE over the sage decreased. At the end of 3 January 1997, there was 357 mm of SWE covering the basin, but the percentages for each vegetation class essentially remained the same relative to the previous day.

At the start of the event, SWE in the exposed areas represented only 3% (86 mm) of the basin total, in the sheltered areas 18% (434 mm), in the drift areas 44% (1160 mm) and in the rest of the basin 35% (261 mm). The exposed and non-drift non-sheltered areas held substantially less SWE than the basin area (3% SWE vs 14% area, and 35% SWE vs 54% area, respectively). Drift areas held substantially more SWE than basin area (44% SWE vs 14% area).

By 2 January 1997, when SWE was at its minimum over the basin, all SWE in the exposed areas of the basin had been depleted, sheltered areas held 21% of the basin total (417 mm), drift areas 50% (1147 mm) and the rest of the basin 28% (177 mm). During the event, drift and sheltered areas maintained or slightly increased SWE, SWE in exposed areas was completely depleted and SWE in the rest of the basin was substantially reduced. At the end of 3 January 1997, a small amount (8 mm) of SWE had been deposited over the exposed areas, but the percentages of basin-wide SWE for each wind-exposure class did not change.

Table 4 presents simulated WAR by vegetation and accumulation/exposure classes for the four primary days of the rain-on-snow event (30 December 1996 through 2 January 1997). The numbers in parentheses next to the WAR values indicate the direct contribution to WAR from rain during that day.

During the first 2 days of the event (30 and 31 December 1996), 55 mm of WAR was simulated, which was dominated by snowmelt. Only 7 mm of this WAR was from rain passing through the snow cover, while 48 mm was from snowmelt. On 1 January 1997, 76 mm of WAR was simulated over the basin, with 45 mm from rain and 31 mm from snowmelt. On 2 January 1997, all 14 mm of simulated WAR was from rain.

Table 4. Simulated WAR by vegetation and wind-exposure class, rain-on-snow event, 30 December 1996 through 2 January 1997, RME sub-basin

	30 Dec.	*31 Dec.*	*1 Jan.*	*2 Jan.*	*Storm totals*	
Conifer (12%)	7 (0)	18 (0)	55 (46)	13 (13)	93 (59)	8%
Aspen (22%)	11 (1)	31 (7)	73 (48)	15 (15)	130 (71)	20%
Sage (66%)	16 (2)	49 (6)	80 (44)	13 (13)	158 (72)	72%
Exposed (14%)	27 (2)	77 (5)	48 (34)	11 (11)	163 (52)	16%
Sheltered (17%)	6 (1)	15 (4)	46 (37)	10 (10)	77 (52)	9%
Drift zone (15%)	3 (1)	22 (12)	99 (87)	22 (22)	146 (122)	15%
"The rest" (54%)	16 (1)	46 (6)	85 (37)	13 (13)	160 (57)	60%
RME basin (100%)	14 (1)	41 (6)	76 (45)	14 (14)	145 (67)	

Notes: Figures in parentheses by the class labels indicate the percentage of the area of RME occupied by that class. Other values in parentheses indicate the amount of the total WAR for that day that was rain either directly on bare ground, or that passed directly through the snow cover.

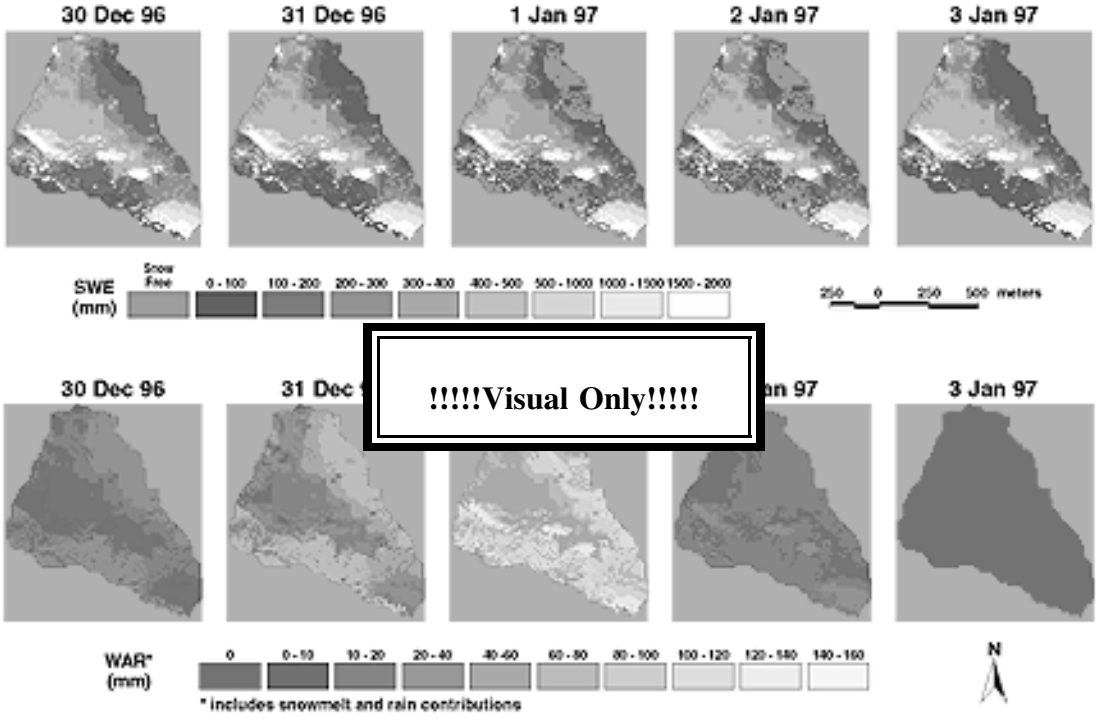

Fig. 2. SWE and WAR at day's end, from the snow cover over the RME sub-basin, 30 December 1996 through 3 January 1997.

In general, the vegetation classes generated WAR that was proportional to area. Conifer areas generated somewhat less WAR, and sage areas somewhat more. The proportion of WAR from snowmelt was 36% in conifer areas, 45% in aspen areas and 55% in sage areas. Most of the sage areas had been depleted of snow by 1 January.

Over the 4 day period of the event, accumulation/exposure classes also generally generated simulated WAR that was proportional to the area each represented. However, this masks the fact that 68% of the WAR from exposed areas and 64% from the rest of the basin was from snowmelt, while only 33% of the WAR from sheltered areas and 16% from drift areas was from snowmelt.

Figure 2 presents simulated patterns of SWE and WAR over the RME sub-basin for 30 December 1996 through 3 January 1997. Areas of zero SWE are shown as green, while areas of zero WAR are shown as red. SWE is scaled from 0 to 1800 mm and WAR from 0 to 80 mm, increasing from black to white.

In the 30 December 1996 SWE image, drift areas show clearly as white, while exposed areas show as dark. Most of the forested areas (conifer and aspen) show as grey regions in the lee of the drift areas. Only minimal WAR was generated on 30 December, with areas of no WAR generation (red areas on the the 30 December WAR image) occurring primarily in the drifts due to the low winds and very deep snow cover at drift sites.

On 31 December, significant WAR is generated, as portions of the exposed areas are depleted of snow. On 1 January, substantial WAR is generated and by the end of the day most of the exposed areas have been depleted of snow. By 2 January, all of the snow in the exposed areas has been depleted, with only minimal WAR being generated. By 3 January, the snow cover has been re-established over the RME basin, as colder temperatures and snowfall have eliminated all snowmelt and generation of WAR.

DISCUSSION AND CONCLUSIONS

It is difficult to determine the accuracy of the spatial estimates of SWE and generated WAR because measured values of SWE were only available at a single point within the basin and measured discharge at the weir integrates many of the basin processes. However, the comparison of measured SWE at the forested RMSP site to SWE simulated over the same vegetation class (conifer) shows similar initial and final conditions, indicating that simulated SWE beneath conifers closely matches measured SWE beneath conifers. Comparison of measured discharge at the weir to simulated basin-wide WAR shows an expected discharge response to the WAR input during the event. The lag in discharge due to soil retention is removed as the time-scale of the analysis is increased. Over the months of January and February, there is reasonable agreement between total simulated WAR (166 mm in January, 26 mm in February, for a 2 month total of 192 mm) and total stream discharge from the RME sub-basin (120 mm in January, 38 mm in February, for a 2 month total of 158 mm).

While vegetation type does influence both the development and melting of the snow cover, in the RME sub-basin this influence is not as significant as topographically induced wind exposure. Differences in SWE occur with vegetation type, but these are smaller, ranging from 164 mm prior to and 227 mm after the event between conifer and sage. In contrast, different wind exposures ranged from 1074 mm prior to and 1178 mm after the event between drift areas and exposed areas. The most significant deposition differences are between wind-exposed areas, which represent 14% of the basin but accounted for only 3% of the basin SWE prior to the event and 0% after the event, and drift areas, which represent 15% of the basin but accounted for 44% of the basin SWE prior to the event and 50% after the event.

Basin-wide, 54% of the simulated WAR during the event was from snowmelt. Most of this came from the

wind-exposed areas and those areas of the RME basin that were not sheltered or in drift zones. Though the drift areas generated a significant amount of WAR during the event (15%), only a small proportion of this was from snowmelt. Wind-exposed, non-sheltered and non-drift areas generated 90% of the snowmelt during the event.

This experiment shows that if the forcing inputs of climate, particularly wind and precipitation, are corrected for terrain and vegetation canopy effects, both snow deposition and melt can be accurately simulated, even during a rain-on-snow event. During this event, snowmelt combined with rain to significantly enhance WAR. Most of the snowmelt was generated over wind-exposed, non-sheltered and non-drift areas. While drifts account for only a small proportion of the snowmelt during the rain-on-snow event, they represent a significant source of SWE and potential WAR for later in the spring.

ACKNOWLEDGEMENTS

We gratefully acknowledge the assistance of D. Robertson and S. van Vactor for collecting, processing and checking meteorological and snow data from the field sites. The information in this paper has been funded by the USDA ARS, with support from the National Resources Conservation Service National Water and Climate Center (Agreement 60-5362-6-223) and the U.S. Army Corps of Engineers Cold Regions Research and Engineering Laboratory (Agreement 000-0A-5362-332). It has been subject to ARS review and approved for publication. Mention of trade names or commercial products does not constitute endorsement or recommendation for use.

REFERENCES

Anderson, E. A. 1976. A point energy and mass balance model of a snow cover. *NOAA Tech. Rep.* NWS-19.

Colbeck, S. C. 1982. An overview of seasonal snow metamorphism. *Rev. Geophys. Space Phys.*, **20**(1), 45–61.

Colbeck, S. C. *and 6 others*. 1979. Snow accumulation, distribution, melt and runoff. *EOS*, **60**(21), 465–468.

Davis, R. E., J. Dozier, E. R. LaChapelle and R. Perla. 1985. Field and laboratory measurements of snow liquid water by dilution. *Water Resour. Res.*, **21**(9), 1415–1420.

Dozier, J. 1980. A clear-sky spectral solar radiation model for snow-covered mountainous terrain. *Water Resour. Res.*, **16**(4), 709–718.

Dubayah, R., J. Dozier and F. Davis. 1990. Topographic distribution of clear-sky radiation over the Konza Prairie, Kansas. *Water Resour. Res.*, **26**(4), 679–691.

Dunne, T. and R. D. Black. 1971. Runoff processes during snowmelt. *Water Resour. Res.*, **7**(5), 1160–1172.

Link, T. and D. Marks. 1999a. Distributed simulation of snowcover mass- and energy-balance in the boreal forest. *Hydrol. Processes*, **13**(14), 2439–2452.

Link, T. and D. Marks. 1999b. Seasonal snowcover dynamics beneath boreal forest canopies. *J. Geophys. Res.*, **104**(D22), 27,841–27,858.

Male, D. H. and R. J. Granger. 1981. Snow surface energy exchange. *Water Resour. Res.*, **17**(3), 609–627.

Marks, D. and J. Dozier. 1979. A clear-sky longwave radiation model for remote alpine areas. *Arch. Meteorol. Geophys. Bioklimatol., Ser. B*, **27**(23), 159–187.

Marks, D. and J. Dozier. 1992. Climate and energy exchange at the snow surface in the alpine region of the Sierra Nevada. 2. Snow cover energy balance. *Water Resour. Res.*, **28**(11), 3043–3054.

Marks, D., J. Kimball, D. Tingey and T. Link. 1998. The sensitivity of snowmelt processes to climate conditions and forest cover during rain-on-snow: a study of the 1996 Pacific Northwest flood. *Hydrol. Processes*, **12**(10–11), 1569–1587.

Marks, D., J. Domingo, D. Susong, T. Link and D. Garen. 1999. A spatially distributed energy balance snowmelt model for application in mountain basins. *Hydrol. Processes*, **13**(13–14), 1935–1959.

Marks, D., A. Winstral, S. van Vactor, D. Robertson and R.E. Davis. In press. Simulating snow deposition, energy balance and melt in a semi-arid watershed. *In Remote sensing and hydrology 2000*. Wallingford, Oxon., IAHS Press. International Association of Hydrological Sciences.

Orme, A. 1989. The nature and rate of alluvial fan aggradation in a humid temperate environment, northwest Washington. *Phys. Geogr.*, **10**(2), 131–146.

Robins, J. S., L. L. Kelly and W. R. Hamon. 1965. Reynolds Creek in southwest Idaho: an outdoor hydrologic laboratory. *Water Resour. Res.*, **1**(3), 407–413.

Seyfried, M. S. and G. N. Flerchinger. 1994. Influence of frozen soil on rangeland erosion. *In* Blackburn, W. H., G. E. Schuman and F. B. Pierson, Jr, *eds. Variability in rangeland water erosion processes*. Madison, WI, Soil Science Society of America, 67–82.

Seyfried, M. S., B. P. Wilcox and K. R. Cooley. 1990. Environmental conditions and processes associated with runoff from frozen soils at Reynolds Creek watershed. *CRREL Spec. Rep.* 90-1, 125–134.

Shanley, J. B. and A. Chalmers. 1999. The effect of frozen soil on snowmelt runoff at Sleepers River, Vermont. *Hydrol. Processes*, **13**(12–13), 1843–1857.

Susong, D., D. Marks and D. Garen. 1999. Methods for developing time-series climate surfaces to drive topographically distributed energy- and water-balance models. *Hydrol. Processes*, **13**(12–13), 2003–2021.

Winstral, A. 1999. Implementation of digital terrain analysis to capture the effects of wind redistribution in spatial snow modeling. (M.Sc. thesis, Colorado State University.)